PROPULSION SYSTEMS FOR HYPERSONIC FLIGHT

C. Segal

University of Florida, Gainesville, Fl, 32611, US

1. Introduction

Given the broad range of aerothermodynamic conditions experienced during flight over the altitude-velocity envelope that is experienced by a scramjet-equipped vehicle it is likely that the scramjet operation will be combined with other propulsion modes. Furthermore, as the flight speed increases the vehicle aerodynamic characteristics and the engine performance become closely coupled; the vehicle forebody becomes part of the engine intake and the vehicle aft becomes part of the engine nozzle; engine throttling changes the pressure distribution on the lower part of the fuselage to a significant degree modifying the moments acting on the vehicle. These considerations include not only the structure of the flowfield generated on the forebody of the vehicle, which is substantial given the low angle of high Mach shock waves, but also the cooling requirements which become increasingly higher with the flight speed and must be assisted by the fuel present on board. This close coupling between engine and the structure requires that, in fact, the selection of the engine cycle will be dictated by the entire system optimization.

Performance based differences between the different engine cycles are clearly illustrated in the fuel specific impulse, $I_{sp} = \frac{Thrust}{Gravimetric\ fuel\ rate}$, diagram shown in Figure 1 (after Billig, 1996a). The diagram shows that around Mach 3 flight regime the subsonic combustion ramjet becomes more efficient as a propulsive system in comparison with the turbine based engines (turbojets of turbofans) but beyond Mach 5 its specific impulse decays rapidly and the scramjet delivers a higher specific impulse at higher speed. The rocket's specific impulse is considerably lower than the other propulsion system but it offers operation capabilities from sea-level static to beyond the atmosphere which no other propulsion system mentioned here can do. The low specific impulse in comparison with the other propulsion systems clearly eliminates the rocket from consideration for long range cruise but as the Mach number continues to increase in the hypersonic regime the scramjet specific impulse approaches that of the rocket engine. Since the very high Mach numbers are expected for operation close to the edge of the atmosphere the continually decreasing air density will eventually require that the engine makes the transition to rocket operation for orbit insertion. Historically, multiple-staged vehicles have been designed to operate with a single type of propulsion system for each stage. Stages are optimized for different altitude/Mach number regimes in the trajectory, increasing the overall system specific impulse. As an example, NASA's hypersonic aircraft demonstrators, X-43, use subsonic aircraft propulsion as the first stage followed by a second stage provided by a Pegasus (first stage) rocket with the scramjet-based

Paper presented at the RTO AVT Lecture Series on "Critical Technologies for Hypersonic Vehicle Development", held at the von Kármán Institute, Rhode-St-Genèse, Belgium, 10-14 May, 2004, and published in RTO-EN-AVT-116.

research vehicle as the third stage. This limited-range accelerator begins its autonomous flight at $M > 7$.

Clearly, the optimization for long range, broad speed regime operation requires the use of a combination of some of these propulsion systems, referred to as combined cycle propulsion (CCP) systems, which not only adapt to the flight regime but also achieve a synergistic performance enhancement over individual cycles. Combined-cycle propulsion systems, which are discussed in more detail below, in section 5, can be broadly divided into two categories: turbine-based combined-cycles that could include turbojet or turbofan cycles, and combined-cycle systems that include a rocket subsystem. Airbreathing combined-cycle engines are intended primarily for missions involving high-speed cruise in the atmosphere with capability to reach orbit by completely switching to rocket mode operation. The requirements for a short duration flight at hypersonic speed can be satisfied with staging.

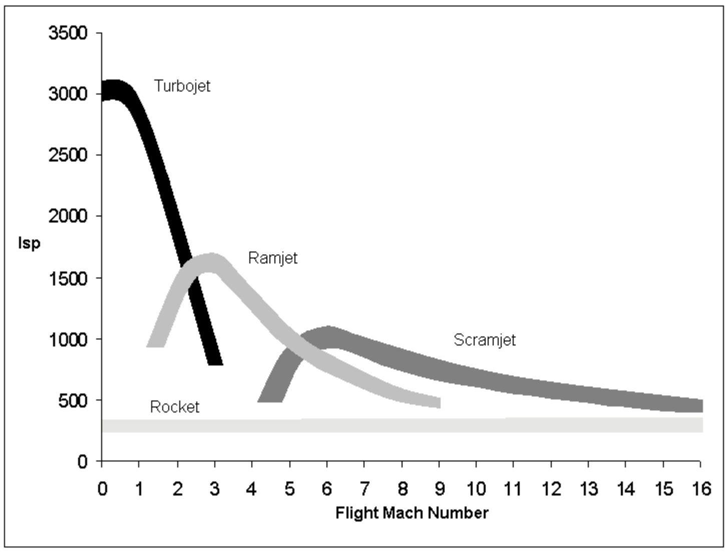

Figure 1. Specific impulse as a function of the flight Mach number for selected engine cycles.

The following sections include generalized discussions of scramjet cycle analysis, performance and integration of the scramjet engine with the vehicle and in combination with other propulsion systems. Component analyses and integration are not included in this discussion.

2. Ideal Scramjet Cycle

The scramjet engine belongs to the family of Brayton cycles which consists of two adiabatic and two constant pressure processes (Mattingly et al, 2002). A simplified schematic of a scramjet engine is shown in Figure 2 describing a lifting body with the vehicle's forebody contributing to a large extent to the inlet compression and the afterbody constituting part of the engine nozzle. The engine, therefore, occupies essentially the entire lower surface of the vehicle. The standard engine designation, which was adopted here after Heiser and Pratt (1994), derives from the standard station designation of gas turbine engines and is used to emphasize the separation between the major engine components:

- station 0 represents the freestream condition,
- station 1 represents the beginning of the compression process. Hypersonic shock waves angles are small resulting in long compression ramps (or spikes for an axisymmetric configuration) which, in many suggested configurations, begin at the leading edge of the vehicle. Additional compression takes place inside the inlet duct.
- station 2.1 represents the entrance into the isolator section. The role of the isolator is to separate the inlet from the adverse effects of pressure rise due to combustion in the combustion chamber. The presence of a shock train in the isolator contributes to further compress the air before entering the combustion chamber. Thermodynamically the isolator is not a desirable component, since it is a source of additional pressure losses, increases the engine cooling loads and it adds to the engine weight. However, operationally it is needed to include a shock train that adjusts such that it fulfills the role described above.
- station 3 is the combustion chamber entrance. Unlike the turbojet engine cycle, where the air compression ratio is controlled by the compressor settings, in a fixed geometry scramjet the pressure at the combustion chamber entrance varies over a large range depending on the flight regime.
- station 4 is the combustion chamber exit and beginning of the expansion.
- station 10 is the exit from the nozzle and due to the large expansion ratios the entire aft part of the vehicle may be part of the engine nozzle.

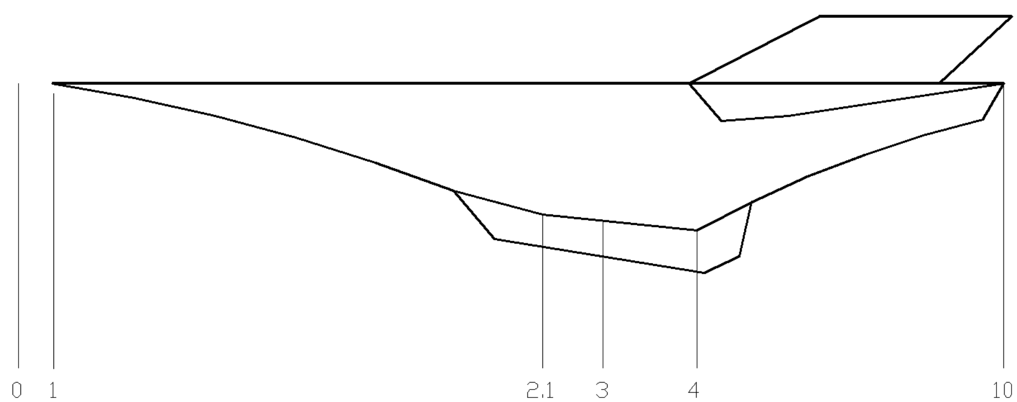

Figure 2. Simplified engine reference stations.

Clearly, this selection of engine stations represents an idealized component separation which omits the presence of additional elements – such as, for example, an MHD generator in the inlet's diffuser coupled with an MHD accelerator in the nozzle's expansion section (Burakhanov et al, 2001) - which may be included in the engine design, or the interaction with other propulsion cycles which, together with the scramjet, constitute a combined-cycle engine.

The engine components' efficiency plays an increasingly significant role as the kinetic energy of the airstream increases. As the flight Mach number increases, the kinetic energy of the air far exceeds the heat released through combustion and, thus, the net thrust becomes only a small fraction of the airstream thrust entering the engine. For example, when flying at Mach 16 using hydrogen in stoichiometric proportion the energy added through combustion is only ¼ that of the airstream kinetic energy (Anderson et al, 2000). The kinetic energy management and it's implications for component efficiency becomes, thus, a critical issue for optimization under the given operational constrains.

The idealized engine cycle can be easily analyzed using the entropic diagram shown in Figure 3. As is the general practice, it is assumed that the air captured by the inlet remains of the same composition throughout the engine and the combustion process

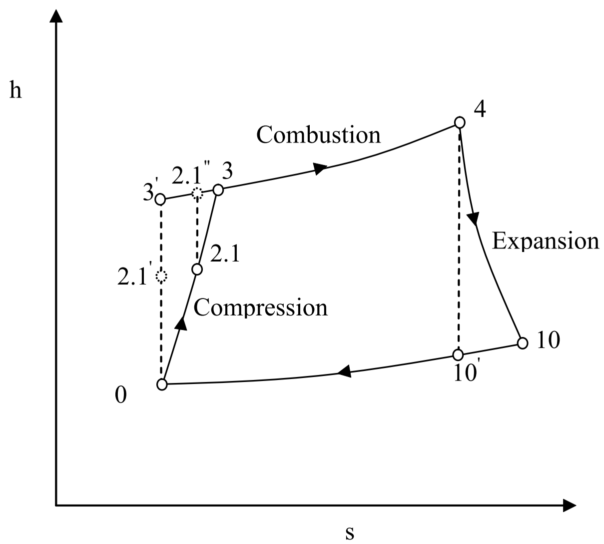

Figure 3. Ideal scramjet cycle. The initial and final thermodynamic states in terms of static specific enthalpy and static specific entropy for each component are indicated by the engine station numbers. Ideal processes are also indicated.

is replaced by heat addition. The additional mass introduced by the fuel is small compared with the air mass flow and can, therefore, be neglected without introducing significant errors in the cycle analysis. Finally, a constant pressure transformation is introduced to close the cycle and return to the original thermodynamic state. These processes are described in some detail below.

The compression process from station **0** to station **2.1** is achieved by flow deceleration through a system of shock waves generated on the forebody upstream the inlet capture through what is referred to as external compression and continues inside the duct through internal compression. Along the forebody a substantially thick boundary layer forms and, since the engine cannot be displaced from the vehicle to avoid boundary layer ingestion or the negative effects of shock-wave/boundary layer interactions which can lead to separation, some of the incoming boundary layer may be removed through air bleed. These quantities of air are, however, small, and their effect on the thermodynamic evolution during compression can be neglected in the entropic diagram.

The degree of flow deceleration in the inlet is dictated by the constraints of velocity and static temperature at the combustion chamber entrance while ensuring,

(i) high efficiency and,

(ii) matching with additional flow streams that may be present in a combined-cycle engine.

The inefficiencies of the compression process, which appear in the entropic diagram as a departure from the isentropic compression, depend on the kinetic energy transformation and its level at the end of the compression process and have obvious implications on the efficiency of the other engine components and the system as a whole. Most notably the static temperature rise due to inefficiencies in the inlet may lead to dissociations that reduce the amount of heat released during the combustion process. Finally, the compression process is influenced by the interactive processes resulting from complex, three-dimensional fluid dynamic interactions that include, in general, multi-angled shock waves, interaction between shock waves and boundary layers, separation vortices and vortex-vortex interactions. Certain designs have suggested addition of fuel during compression in the inlet to increase the residence time for improved mixing (Guoskov, 2001and Vinogradov, 2001), therefore introducing mass, changing the properties of the incoming air and affecting the inlet kinetic efficiency.

The level of flow distortions generated in the inlet, both steady-state and dynamic, has a clear effect on the heat release processes in the combustion chamber through distortions interaction with mixing and turbulence/temperature effects (Warnatz, 1996, Oran and Boris, 2001). Inlet flow distortion effects on the compressors in turbojet engines have been studied and documents extensively (Younghans, 1989), however, the effect of inlet distortions in ramjet/scramjet engines have not been evaluated sufficiently to date.

The process in the isolator, between stations **2.1** and **3** can be considered part of the compression process although the isolator has the clearly defined function to protect the inlet flow from the pressure changes in the combustion chamber. This compression is the result of the shock train present in the isolator which, depending on the flight regime, may extend into the core of the combustion chamber surrounded by regions of subsonic flow or end with a normal shock thus rendering the entire flow subsonic before arriving at the combustion chamber. The inefficiencies in the isolator result from viscous losses, heat lost to the walls and shock/boundary layer interactions.

The diagram shown in fig. 3 includes the idealized isentropic compression in the inlet between states 0 and $2.1^{'}$ and the isentropic isolator compression between states 2.1 and $2.1^{''}$.

Between stations **3** and **4** heat is released through fuel combustion. Assuming, in a first approximation (Heiser and Pratt, 1994), that the enthalpy remains constant between the free stream and the entrance to the combustion chamber, i.e., station 3, a relation between M_3 and M_0 can be written, which, in the limit of large flight velocities, of the order of M_0 =10, becomes,

$$\frac{M_3}{M_0} \approx \sqrt{\frac{T_0}{T_3}} \tag{1}$$

Since the expected temperature ratios T_3/T_0 are of the order of 10, equation 1 implies that the compression in the inlet-isolator results in M_3 approximately one-third of M_0.

The departure from constant stagnation pressure in the combustion chamber is due mostly to friction, Rayleigh losses and heat transferred to the wall (Heiser and Pratt, 1994). The amount of heat released within the combustion chamber depends on the efficiency of the mixing process and the degree of conversion of the available chemical energy into sensible energy. Following some sort of flameholding scheme the combustion chamber is usually designed with a constant area for rapid heat release followed by a slowly expanding region to delay the onset of thermal choking which is particularly severe at low speed operation. At high speed this slowly diverging section acts as an initial expansion region in which the flow has additional time to reach chemical equilibrium (Ortwerth, P.J., 2000).

Expansion follows between stations **4** and **10,** first in an internal nozzle and continues on the vehicle aft to, ideally, perfect expansion. The irreversibilities in the nozzle are caused by friction, viscous dissipation through shocks and heat lost to the structure. If rapid expansion begins before the chemical equilibrium has been achieved at the exit from the combustion chamber a certain amount of dissociated species may freeze leading to additional energy loss. The degree of expansion results from the optimization of engine performance, vehicle dimensions and the requirements to balance the moments for trimmed flight.

Finally, the cycle is completed with the imaginary process from **10** to **0**, which represents heat rejection at constant pressure, equivalent with the difference between the thermodynamic conditions at the nozzle exit and the freestream.

This is a grossly simplified representation of the scramjet thermodynamic cycle. It is expected that the scramjet will operate with other propulsion systems in a combined cycle so that the propulsion system/vehicle can be optimized for the entire flight regime. The corresponding thermodynamic cycle will differ from the ideal cycle presented here, according to the engine configuration selected. Some of these cycles are reviewed below in section 5.

3. Trajectory and Loads

Optimization of the scramjet powered vehicle trajectory takes into account the mission requirements, such as insertion into low earth orbit (LEO) using airbreathing propulsion for the transatmospheric flight (Hargraves and Paris, 1987) or a more restrictive mission for hypersonic missiles (Bowcutt, 2001), within the constraints dictated by size, structural loads and operational features such as the transition from the initial propulsion cycles to scramjet and than to strictly rocket propulsion.

Possibly the most critical mission parameter is the maximum payload and can be maximized, largely, by minimizing the fuel consumption. Therefore, an optimal trajectory may be inferred from energy-altitude analyses (Bryson et al., 1969, Schmidt, 1997) in which global minimization of fuel consumption results from a maximization of the energy level with respect to fuel consumption, $dE\big/dW_{fuel}$. Under the energy-state assumption (Schmidt and Herman, 1998) the energy change with respect to fuel consumption can be related to the flight conditions, i.e., thrust, T, drag, D and specific impulse I_{sp},

$$\frac{dE}{dW_{fuel}} = \frac{VI_{sp}}{W}\left(1-\frac{W}{T}\frac{D}{L}\right) \tag{2}$$

and contours of constant dE/dW_{fuel} can be sketched on an altitude-velocity map. The loci of the curves maxima describe an optimal trajectory with respect to the minimum fuel consumption which has been selected as the optimization parameter in this case. Similarily, the trajectory can be optimized with respect to the optimal time to reach a desired altitude, with the time to change the altitude obtained from

$$\Delta t = \int_{E_1}^{E_2} \frac{dE}{dE/dt} = \int_{E_1}^{E_2} \frac{W}{(T-D)V} dE \tag{3}$$

The optimized trajectory for one of these two conditions can be maintained as long as the constraints in the system are satisfied, including (i) energy addition through combustion and (ii) the dynamic pressure limit.

On the same basis of kinetic energy of the air ingested by the scramjet engine and under the constraint of energy availability from the fuel on board Czysz and Murthy (1995) separated the scramjet engine operation in five regimes depending on the flight velocity. These regimes reflect, in the order of increasing flight velocity, the ability to add energy to the air through combustion which works in competition with the engine drag losses. Figure 4 shows these regimes on a typical flight trajectory corridor. At moderate hypersonic flight velocities a significant amount of heat can be added to the airflow while the engine drag losses are relatively moderate resulting in high vehicle acceleration. The situation gradually changes as the relative heat addition to the air progressively decreases with increased flight velocity whereas the drag losses (Riggins, 1997, Mitani, 2002) continuously increase until the heat addition can no longer overcome the drag and the airbreathing based system reaches the limit of its flight envelope.

Optimizations of vehicle architecture under the constraints of thermal and mechanical loads, external drag and internal irreversibilities have generally indicated in recent studies (Mehta and Bowles, 2001, Trefny, 1999) that trajectories for both single and two-stage-to-orbit concepts are limited to a flight dynamic pressure residing between 4500 – 9000 kg/m^2 (about 1000 – 2000 lb/ft^2). The lower values are needed to reduce the aerodynamic drag during the transonic flight transition and the higher values are recommended for the hypersonic acceleration.

A typical trajectory corridor is shown in Figure 4 which includes the range of altitude-Mach numbers experienced during the flights with the experimental Kholod vehicle in the early ’90 (Semenov, 2002). Higher dynamic pressure ratios are expected during the re-entry from orbital flight and deceleration when drag is used to dissipate the kinetic energy. Also included in this figure are the estimates of energy added by combustion as a percentage of the airstream energy as the flight Mach number increases (Czysz and Murthy, 1995). These ratios indicate that around Mach 25 the scramjet engine reaches an energetic operational limit.

4. Performance Analysis

In the Breguet range equation,

$$R = V \cdot I_{sp} \left(L/D \right) \ln \left(W_0/W_f \right) \tag{4}$$

where, W_0/W_f is the ratio of the vehicle weights at the beginning and the end of the cruise segment and V is the flight speed, the $V{\cdot}I_{sp}$ term is essentially constant for a scramjet engine in the domain of hypersonic flight regime (Ortwerth, 2000). The vehicle will be, thus, required to fly at the best L/D and the product $V{\cdot}I_{sp}$ will have to be maximized. This parameter depends on the propulsive efficiency, the efficiency of the chemical to thermal energy conversion in the combustion chamber and the efficiency of the other thermodynamic processes in the engine components.

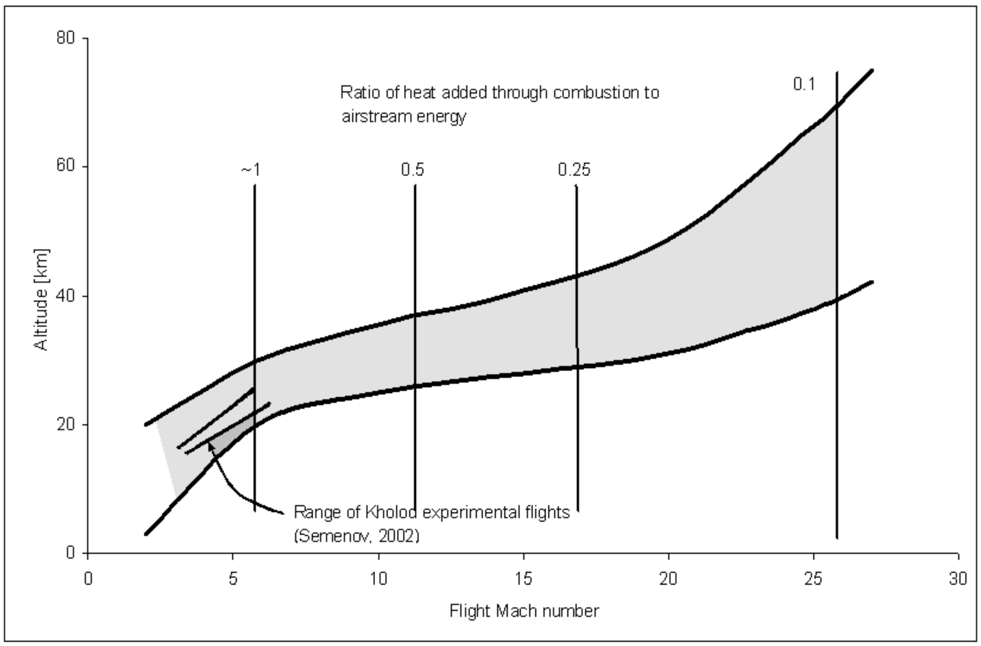

Figure 4. Flight regimes indicating the ability to add energy through combustion and the limit of thrust production (after Czysz and Murthy, 1995)

Through the analysis of the scramjet cycle shown in fig. 3, the nozzle exit velocity is obtained as,

$$V_{10}^2 = V^2 + 2H_0(\psi - 1)\left[\eta_c \eta_e \left(\frac{\Delta H_c / H_0}{\psi} \right) - 1 \right] \tag{5}$$

where, H_0 is the flight enthalpy, ΔH_c is the energy added through chemical reactions, η_c and η_e are the inlet compression and nozzle expansion thermodynamic efficiencies, respectively. These two efficiency terms are defined as the departure of the compression and the expansion static enthalpy changes during each of these processes from the equivalent adiabatic evolution between the same isobars, i.e.,

$$\eta_c = \frac{h_{3'} - h_0}{h_3 - h_0} \quad and \quad \eta_e = \frac{h_4 - h_{10}}{h_4 - h_{10'}} \tag{6}$$

The parameter ψ in the specific impulse equation represents the inlet static enthalpy rise through compression, $\psi = {}^{H_3}\!/_{H_0}$ and is limited by the maximum allowable compression temperature determined from considerations of dissociation. Thus the specific impulse defined as the thrust-to-massflow ratio becomes,

$$I_{sp} = \frac{F}{\dot{m}g} = \frac{1}{g}(V_{10} - V) = \frac{V}{g}\left\{\sqrt{1 + \frac{2}{(\gamma - 1)M_0^2}(\psi - 1)\left[\eta_c\eta_e\left(\frac{\Delta H_c / H_0}{\psi}\right) - 1\right]} - 1\right\} \tag{7}$$

where H_0 / V^2 has been simplified under the assumption that the air behaves as a thermally perfect gas and the flight Mach number has been emphasized.

Notable in this equation are the compression and the expansion efficiencies. Implicitly, the specific impulse equation contains the combustion efficiency defined as,

$$\eta_b = \frac{\Delta H_c}{fH_f} = \frac{H_4 - H_3}{fH_f} \tag{8}$$

where f is the fuel-to-air massflow ratio and H_f is the fuel heating capacity through the term ΔH_c. The combustion efficiency depends on the geometric configuration of the combustion chamber and the air and fuel thermodynamic properties entering the combustion chamber and is closely coupled with the efficiency of the mixing process. Thus, equation 7 emphasizes the effects of the components efficiencies on the specific impulse, a key parameter in the vehicle trajectory and sizing optimization.

It would appear from equation 7 that the efficiencies of these three components, the inlet-isolator group, η_c, the combustion chamber, η_b, and the nozzle, η_e, have the same quantitative effect on the specific impulse. Yet, lower compression efficiency leads to an increased temperature T_3 which reduces the amount of heat that can be released in the combustion chamber therefore changing the mixing and combustion efficiencies and, by modifying the thermodynamic properties at the end of the combustion process influences the expansion in the nozzle and the efficiency of this process. For this reason, thermodynamic cycle analyses based on individual components in sequence provide only qualitative results.

From the point of view of the cycle thermodynamic analysis it is interesting to draw the attention to other global parameters of engine efficiency, in particular the propulsive efficiency which is defined as the engine exit energy realized out of the total energy available (Bullock, 1989). With the assumption that there is no mass change throughout the engine, the propulsive efficiency becomes,

$$\eta_p = \frac{2V_0}{V_{10} + V_0} \tag{9}$$

This parameter would indicate that the maximum propulsive efficiency is obtained when the nozzle exit velocity equals the flight velocity, a condition when, evidently, no specific impulse is created.

The propulsive efficiency is often combined with a thermal efficiency, η_{th}, which is defined as the kinetic energy increment across the entire engine with respect to the amount of energy contained in the fuel consumed:

$$\eta_{th} = \frac{\frac{1}{2}\left(V_{10}^2 - V^2\right)}{fH_f} \tag{10}$$

The engine thermal efficiency is similar to the definition of the combustion chamber efficiency but it incorporates all the engine components. Therefore, energy not released in the combustion chamber due to inefficiencies of the mixing and combustion processes still appears the engine thermal efficiency defined as above.

5. Combined Cycles

One method to avoid expendable staging and make use of more efficient engine cycles during part of the ascent to orbit is the of two or more propulsion systems that operate independently. These are referred to as combination propulsion systems (CPS). An example of this type of propulsion system is a combination of rocket and ramjet which uses a rocket booster to achieve the initial acceleration to speeds capable of sustaining the ramjet operation (Billig, 1996a) when the engine switches entirely to ramjet operation for the remainder of the flight. Although the use of CPS avoids propulsion systems integration issues, it requires carrying at all times at least one propulsion system that is not actively contributing to thrust generation and, thus, leads to inefficient use of weight, volume and increases the heating load.

Another way to use high-efficiency airbreathing cycles during ascent in a reusable system is through the use of combined cycle propulsion (CCP) systems. Combined-cycle propulsion systems can be broadly divided into two categories: airbreathing combined-cycles that could include turbojet or turbofan cycles, and combined-cycle systems that include a rocket subsystem. Examples of airbreathing CCP systems are the dual mode combustion ramjet, which operates in both ramjet and scramjet modes (Curran et al, 1996), and the turbine-based combined-cycle engine, which uses a turbine-based cycle for low-speed flight along with ramjet and scramjet modes (Georgiadis, et al, 1998). Airbreathing combined-cycle engines are intended primarily for missions involving high-speed cruise in the atmosphere, but cannot support transatmospheric flight when the air density becomes to low to sustain the cycle. A rocket based cycle is then needed. The following sections discuss some of the relevant issues for the combined-cycles using ramjet/scramjet architectures in combination with gas-turbine or rocket engines.

5.1 The Turbine Based Combined Cycle - TBCC

The TBCC are particularly attractive for the unsurpassed specific impulse at takeoff. In that regard, the TBCC are of particular interest for TSTO concepts in which the first stage spends most of its mission at relatively low supersonic speed. Recent technological advances concentrate on the development of turbine engine technologies that could operate efficiently up to Mach 4 (Bartolotta et al, 2003).

A simple combined cycle is a turbojet (or turbofan)/ramjet in which a secondary flow bypasses the core turbojet and participates to produce thrust in an afterburner. As the Mach number increases, typically beyond M = 3, the afterburner transitions to operation as a ramjet while the turbojet maximum cycle temperature is reduced to maintain an acceptable load on the rotating machinery while maintaining the airflow path open to contribute to thrust generation in the afterburner. The main issue in this configuration is, evidently, the matching of the core flow with the bypass flow to avoid reversed flow on any of the sides. Additional operational difficulties derive from the broad bypass ratio range during acceleration and deceleration and the thermal management of the moving parts during high enthalpy flight.

An interesting combined cycle including turbojet/rocket interaction is described by the KLIN™ cycle (Balepin et al, 2002) shown schematically in Figure 5. The rocket's

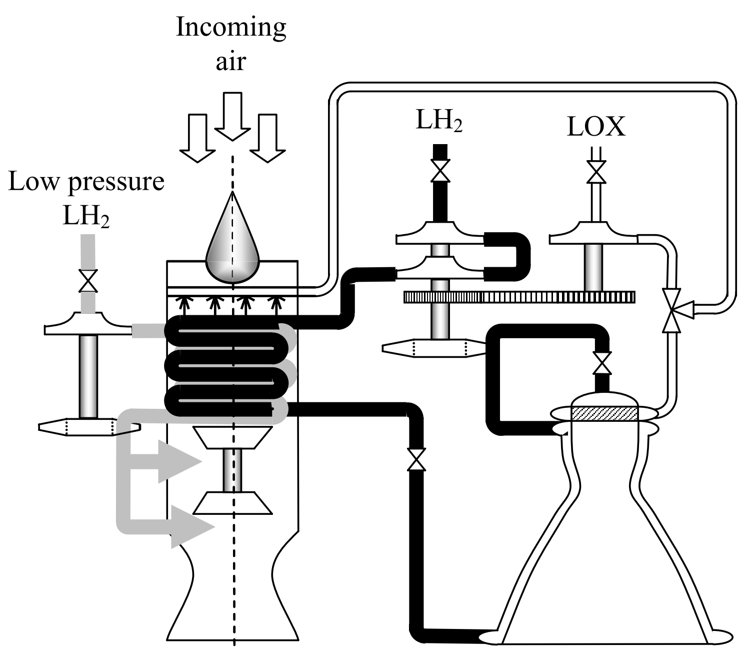

Figure 5. The KLIN™ turbojet/rocket configuration (Balepin et al, 2000) incorporates a deep cooled turbojet cycle along with a liquid fueled rocket. Both the turbojet and the rocket operate with hydrogen as fuel.

fuel, hydrogen at high pressure, is used to provide deep cooling of the air in the turbojet intake. In the diagram in fig. 5 both the rocket and the turbojet use hydrogen as fuel but the two fuel circuits could be completely separated to use non-similar fuels using, for example, liquid hydrocarbons for the turbojet. Although the rocket and the turbojet use different flowpaths there is a close interaction between the cycles since the rocket's fuel is used to cool the turbojet incoming air to increase the density and reduce the temperature, thereby increasing the compression in the turbojet and extending its operation to higher Mach numbers. As the velocity changes both the turbojet and the rocket are throttled to adapt to both the low and the high speed regimes. This system is estimated to have up to Mach 6.5 operational capability.

Although it is not strictly a combined cycle, the liquid air cycle engine (LACE) is a combination of rocket cycles with air collection in flight through an arrangement as shown in Figure 6. The concept involves air collection during initial stages of rocket operation through atmosphere, chilled by liquid hydrogen and the condensed liquid oxygen is later injected in the main engine where it burns with the liquid hydrogen. The propulsion system overall weight is thereby reduced. The concept was included in the design of the British HOTOL program in the mid 1980s (Hallion, 1995).

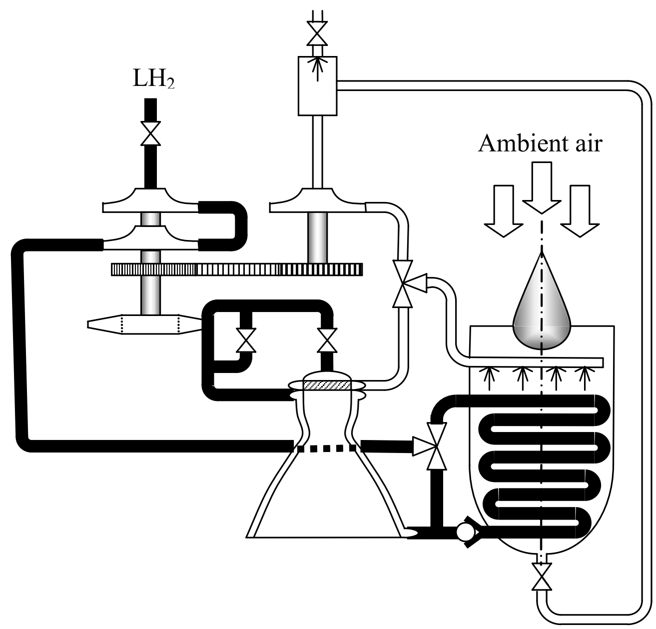

Figure 6. Liquid Air Collection Engine (LACE) concept using mixed air and oxygen oxidizer (Balempin et al , 2000).

5.2 The Rocket Based Combined Cycle - RBCC

Among the many types and variations of CCP systems, one class of rocket-based CCP systems shows particular promise for Earth-to-orbit (ETO) missions. These are engines that operate in rocket-ejector mode and also have the capability of operating in ramjet, scramjet, and rocket-only modes, and are typically referred to as rocket-based combined-cycle (RBCC) engines. One variant is the ejector scramjet engine is shown schematically in Figure 7. This concept has been identified as one of the most promising propulsion system for both single-stage-to-orbit (SSTO) and two-stage-to-orbit (TSTO) vehicles (Escher and Flornes, 1966).

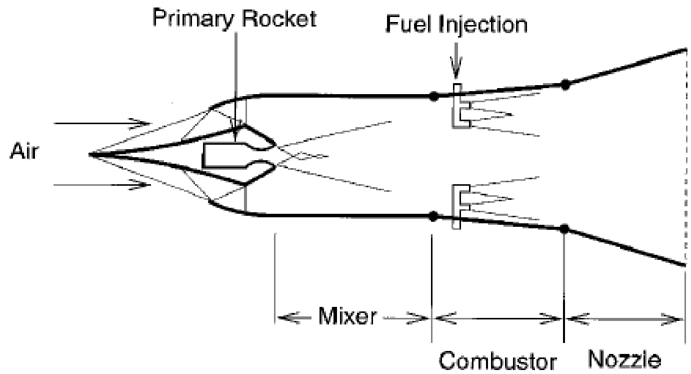

Figure 7. Schematic diagram of a RBCC with a rocket acting as an ejector to augment the airflow into the ramjet/scramjet segment.

The ability to utilize the rocket as an ejector increases the engine mass flow, therefore, thrust. Afterburning in rocket-ejector mode, using the ramjet/scramjet fuel injectors, further increases the thrust and specific impulse compared to the rocket operating alone. As the ratio of the bypass air to the rocket exhaust mass flow increases with increasing flight speed, the specific impulse continues to increase as the cycle more closely resembles ramjet operation. In ramjet and scramjet modes, the rocket could be advantageously used as a fuel injector and mixing enhancer. In the rocket-only mode, the use of the engine duct as a highly expanded nozzle at high altitudes increases the specific impulse of that mode of operation.

A further advantage of RBCC systems is the reduction in the amount of onboard oxidizer required. This decreases the size and, therefore, the weight, of the tank and vehicle. Vehicle propellant mass fractions for RBCC-powered vehicles are projected to be around 70%, as compared to 90% for all-rocket vehicles (Escher et al, 1995). In the rocket-ejector mode, RBCC systems can provide vehicle thrust-to-weight ratios greater than one and are therefore capable of vertical takeoff and landing. Finally, the cryogenic fuel can be used in airbreathing modes as a heat sink to increase the density of the inlet airflow, thus increasing the work output. In terms of the thermodynamic cycle, this is equivalent to a more efficient process between states **0** and **2.1** shown in Figure 3.

5.2.1 RBCC Systems Mode of Operation

As one of the most promising RBCC configurations the ejector scramjet shown in Figure 7 is the basis for an entire class of RBCC engines. It consists of a rocket subsystem incorporated in an airbreathing engine along with an inlet, mixer, combustion chamber and nozzle. Fuel injections sites can be located at several locations along the duct to optimize the fuel injection selection according to the requirements of the flight regime and engine operation. The ejector scramjet operates in the four modes described in Figure 8: rocket-ejector, ramjet, scramjet, and rocket-only mode.

The rocket-ejector mode shown in fig. 8a is an ejector cycle with the rocket acting as the primary or drive-jet. The thrust of the rocket is augmented through a jet pumping process that transfers momentum from the high-velocity rocket exhaust to the inducted air. The ejector process results in an increased total mass flow with a lower exit velocity and yields a higher specific impulse in comparison to the rocket-only operation. The rocket-ejector mode is used from takeoff through low supersonic flight speeds. Specific impulse is typically augmented by 10– 20% at static conditions, and the augmentation increases to levels up to 250% at Mach numbers between 2 and 3.6,9 Much of the thrust augmentation is accomplished in the rocket-ejector mode by afterburning fuel with the inducted air in the duct downstream of the rocket (Dykstra et al, 1997). As the flight Mach number approaches 3, the engine transitions to ramjet mode (fig. 8b) which provides a higher specific impulse in the mid-to high-supersonic flight speed range.

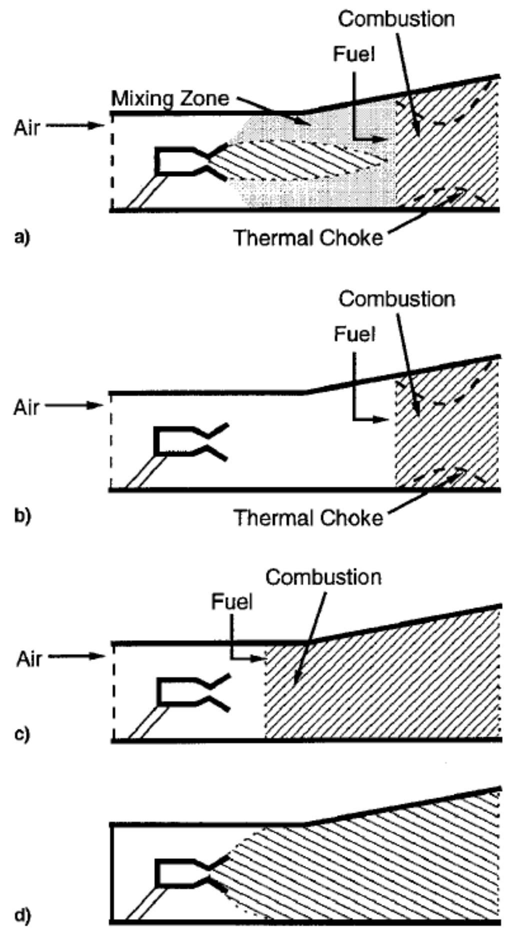

Figure 8. Operation of an ejector scramjet RBCC: a) rocket-ejector, b)ramjet, c)scramjet and, d) rocket-only.

Oxidizer is supplied by the ram air from the inlet, and combustion takes place at subsonic conditions. Around $M = 6$, the operation of the engine is turns to the scramjet mode (Fig. 8c), when the flow remains supersonic throughout the entire engine. The engine combustion cross section must remain constant or diverge in this mode to avoid the onset of thermal choking in the scramjet. The rocket is either turned off or used as a fuel injector in both ramjet and scramjet modes. Around $M = 15$ the air density can no longer sustain an efficient airbreathing cycle and the engine is switched to the rocket-only operation as shown in Figure 8d. The air inlets close and the rocket restarts providing thrust to insert the spacecraft into orbit.

Several extensive studies (Escher and Flornes 1966, Foster et al 1989) evaluated a number of engine configurations for applications including single-stage-to-orbit (SSTO) and two-stage-to-orbit (TSTO) vehicle concepts. Among these configurations the most promising that emerged consisted of the basic ejector scramjet shown in fig. 8a with one or more additional subsystems. For example, the basic ejector scramjet cycle engine shown in Figure 9a can be complemented with a turbofan to supercharge the flow in rocket-ejector mode as shown in fig. 9b, or an air liquefaction subsystem that can produce the necessary oxidizer for the rocket during the flight when the engine operates in rocket-ejector modem as shown in fig. 9c. The latter solution eliminates the need to carry a considerable amount of oxidizer on board resulting in a reduced vehicle weight. These

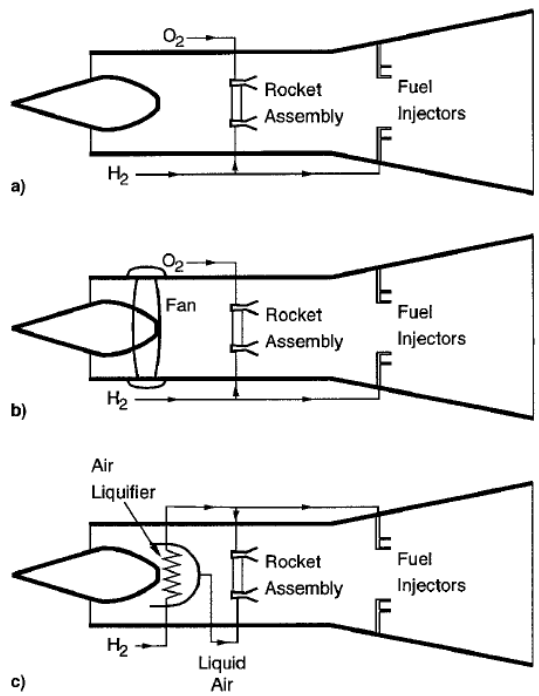

Figure 9. Schematic diagram of subsystems that could be added to an ejector scramjet engine: a) basic ejector scramjet, b) ejector scramjet with turbofan and c) ejector scramjet with air liquefaction system.

engines were found to have overall mission-effective specific impulses between 630 and 780 s, compared with 370 s for a dual-fuel, all-rocket SSTO vehicle (Foster et al, 1966). Along with added capabilities to the engine, these subsystems also present additional design challenges for the successful operation, which are discussed below. Several other vehicles with CCP systems have been analyzed, with applications to both multiple-staged and single-staged vehicles (Billig 1996b, Ganji et al 1991, Sosounov et al 1996, Czysz and Murthy 1995, Esher 1997). These theoretical studies have been accompanied by experimental demonstration of feasibility and mode transitions (Leingang 1992, Siebenhaar 1995).

5.2.2 Combined-Cycle Propulsion Technical Issues

Flow Path Design and Optimization

The advantage of being able to operate in several different cycles in a single engine carries with it the additional requirement of designing a flow path that will provide acceptable performance in each operational mode. The inlet will need to operate with a very low contraction in the rocket-ejector mode to capture as much air as possible (Billig 1993). However, in the scramjet mode it will need to have a large enough contraction to provide sufficient compression of the incoming air before combustion. The optimum exit flow path in rocket-ejector and ramjet modes includes a converging–diverging section, while scramjet mode requires straight and diverging sections only. Variable geometry, while an obvious solution, would add significant weight and complexity to the engine (Rohde 1992). Fixed geometry flow paths are possible through the use of thermal compression and thermal choking to provide an effect analogous to area change in the flow path. Tailoring the fuel injection location and amount is used to alter the flow instead of variable geometry, and requires careful design of the fuel injection system. Fixed geometry inlets using thermal compression were proposed by Ferri in 1973 and significant performance enhancement was shown to be possible at low hypersonic speeds through three dimensional optimization of the compression system (Billig et al, 1968). Newer concepts based on magnetohydrodynamic (MHD) energy extraction in the inlet and redistribution in the nozzle (Burakhanov et al 2001) point as well to the possibility to adjust the inlet flow to the flight conditions without geometrical changes. However, progress on these concepts has been limited by the difficulty involved in tailoring the flow, fuel injection, heat release and vehicle integration (Curran et al 1996). Furthermore, for fixed combustor/nozzle geometry, the flow path would also need to be optimized to allow controllable thermal choking in rocket-ejector and ramjet modes while avoiding thermal choking in scramjet mode.

Fuel Selection and Densification

The issue of fuel system selection is an important integrating factor in the development of high-speed propulsion systems including combined-cycle approaches. It encompasses issues of fuel management, stability, and energy density, along with the need for fast breakup and chemical decomposition of the injected fuel. Often these requirements are in contradiction, because high energy-density fuels require high activation energies to initiate exothermic reactions (Segal and Shyy 1996). For SSTO vehicles, hydrogen provides an overall specific impulse better than hydrocarbon-based fuels because of the higher energy density and provides a source for active cooling of the airframe. In addition, the fast chemical kinetics of hydrogen contribute to reducing the combustion time in the scramjet mode operation. Advances such as gelled hydrogen (Palaszewski et al 1997) or slush hydrogen (Escher, 1992) provide methods to increase the density of hydrogen. Slush hydrogen yields a 15% increase in density compared to liquid hydrogen and, additionally, it provides 20% greater thermal sink. This is important, particularly in the liquid-air cycle engine (LACE) concept where hydrogen "recycling" i.e., returning some hydrogen to the slush hydrogen tank for recooling, can increase the engine performance. For TSTO vehicles, the use of hydrocarbon-based fuels, including some newly formulated synthetic fuels with high energy content (Segal et al 1995), is a possibility. A number of synthetic fuels have been developed recently (Marchand, 1995) that have the potential of an increased gravimetric energy output; hence improving the vehicle mass properties. This category includes energetic fuels, including strained-bond molecules and hydrocarbons with large molecular formulations or those including azido groups, as well as solutions of more traditional formulations with energetic additives. Aspects of the combustion characteristics of several such energetic fuels have been reviewed by Segal and Shyy 1996, Marchand et al 2002, and Yang, V. and Zarko, 1995.

5.2.3 Mode-Specific RBCC Technical Issues

Mixing-Enhancement in Rocket-Ejector Mode

When a single circular cross-sectional centerline-mounted rocket is used for rocket-ejector configurations mixing lengths are large. Experimentally derived correlations for this configuration indicate that a duct length-to-diameter ratio (L/D) of 8 to 10 is required for complete mixing (Dykstra 1997). Decreasing the duct length is important to reduce the engine weight; however, it can not be accepted at the expense of incomplete mixing. Increasing the interfacial shear area between the primary and secondary flows increases mixing and reduces the required length because mixing results primarily from the turbulent and viscous shear forces in steady flow ejectors. Therefore, using a larger number of smaller primary rockets has proven effective in reducing mixing length (Siebenhaar 1995, Gregory and Han 2003). An annular bell rocket has been suggested with a toroidal combustion chamber and an annular nozzle which increases the shear area (Escher and Schnurstein 1993). It has been shown (Daines and Merckle 1995) that an ejector utilizing an annular bell rocket mixes about four times as fast, lengthwise, as an ejector with an on-axis primary jet and it has been estimated that a dual concentric annular bell would have an L/D of about one for complete mixing.

Mixing can also be enhanced in an rocket-injector mode cycle by inducing large-scale motion between the primary and secondary streams, which effectively increases the shear area. Forced mixer lobes (Presz et al 1988) and primary jets with noncircular cross sections (Ho and Gutmark 1987, Kim et al 1998) induce large scale fluid motion through vortex formation. For highly elliptic-shaped jets, the entrainment of secondary fluid on the minor axis is increased by as much as a factor of 8 compared to a circular jet (Liou et al 1993) while the mixing rate on the major axis remains similar to that of a circular jet.

Turbulent mixing, which occurs in steady-flow ejectors, increases the stagnation pressure losses in the flow and results in lower performance compared with theoretical ideal mixing. In contrast, dynamic ejectors rely primarily on unsteady pressure waves to accelerate the secondary flow and accomplish the momentum transfer and can, therefore, perform better than steady-flow ejectors. For example, an intermittent jet ejector (Lockwood and Patterson 1962), where the primary jet is pulsed, resulted in 90% thrust augmentation as compared to 30% augmentation for the corresponding steady-flow ejector. Resonant acoustic modes excited naturally by the primary jet in some ejectors have been correlated with increased mass entrainment (Bowman et al 1990). Other unsteady ejector modes have been suggested to improve mixing including (i) rotary jets, where the primary jets emanating from a freely rotating cylindrical or annular rotor drive the secondary air through the engine (Amin and Garris 1995), and, (ii) switching the rocket exhaust flow from side to side in a planar rocket duct to increased acceleration of the slower secondary air (Bulman 1993); computational results indicated an increase of over 30% in specific impulse and a mass entrainment increase of over 10% at a switching frequency of 500 Hz compared to a steady-flow ejector in the latter configuration (Daines and Bulman 1996). Although dynamic ejectors may prove useful in combined-cycle engines, practical technical issues such as increased weight, induced vibrations, and achieving jet switching must be first resolved.

Simultaneous Mixing and Combustion vs Diffusion and Afterburning

Related to the issue of enhanced mixing is the question of whether to employ diffusion and afterburning (DAB) or simultaneous mixing and combustion (SMC) for the afterburning in the rocket-ejector mode. In the simultaneous mixing and combustion approach fuel-rich rocket exhaust is used to drive the mixer flow and combustion is allowed to occur simultaneously with mixing and expansion. The resulting subsonic flow stream is then passed through a converging– diverging nozzle and expanded to supersonic velocities. An alternative approach is to mix a stoichiometric supersonic rocket drive jet with the subsonic inlet airstream and expand the combined subsonic flowstream to increase the static pressure. At the peak pressure point, additional fuel is introduced and burned and the entire flow is expanded through a converging– diverging nozzle. This approach is referred to as diffusion and afterburning. The SMC cycle exhibits consistently lower engine specific impulse at low Mach numbers relative to DAB cycles, as one would expect from basic thermodynamic consideration governing heat engine cycle efficiency. This difference is significant at sea-level static conditions but diminishes progressively with increasing Mach number. One experimental study (Stroup and Pontzer 1968) showed that combustion efficiency of the afterburner in the rocket-ejector mode decreased from over 90% with DAB to about 40% with SMC by decreasing the length available for mixing before fuel injection. However, an SMC engine with a fuel-rich rocket exhaust has the advantage that separate downstream fuel injection capability is unnecessary, thereby reducing the engine weight and complexity. Billig (1993) has been suggested that a shorter engine duct more than offsets the lower efficiency by a compensatory decrease in engine weight. Furthermore, one suggested method (Siebenhaar and Bulman 1995) to minimize losses is to introduce a fuel-rich flow that is shielded by the rocket exhaust from immediately mixing and allowed to react with the secondary air. This eliminates the need for downstream fuel injection, while allowing improved mixing before afterburning occurs.

Rocket-Only Mode Cycle Efficiency

RBCC systems can make use of the airbreathing duct to act as a high-expansion nozzle when the ambient pressure is low to increase the overall performance. This rocket-only mode of operation has to be considered during the flowpath optimization because a well-designed ramjet or scramjet flowpath does not necessarily result in high efficiency in the rocket-only mode. The study by Steffen et al (1998) evaluated the effect of various parameters, including the engine duct area at the rocket exit plane, rocket nozzle exit area, wall angle and base bleed on the cycle efficiency of an RBCC engine in rocket-only mode operation. Results showed that a large engine duct area at the rocket exit plane and a long engine duct resulted in a decreased the specific impulse while large rocket nozzle exit areas and engine duct exit areas increased the specific impulse. In addition, for a divergent nozzle, base bleed reduced the specific impulse. Depending on the geometry, cycle efficiencies ranged from about 78 to 95% of ideal rocket performance, which was computed assuming a well-designed nozzle with the same overall expansion ratio.

Enhancements to the Basic Ejector Scramjet Configuration

System studies indicated several subsystems could be added to the basic ejector scramjet to increase the specific impulse. One subsystem that improves the specific impulse in the rocket-ejector mode is a turbofan included in the flow path before the rocket as shown in fig. 9b. A turbofan adds the capability of powered loiter with substantially increased specific impulse, as high as 23,000 by some estimates (Escher 1997). However, these advantages come at the expense of increased installed weight and complexity. A major issue with this option is the removal of the rotating machinery from the flow path and stowage during elevated-Mach number flight to protect it from the extreme temperature conditions that would be experienced. Several methods have been suggested, including swinging or rotating the fan out of the flow path (Escher 1997).

A method suggested to increasing the specific impulse in a rocket-ejector mode at the expense of extra weight is to include a liquid air cycle engine (LACE) subsystem, shown schematically in fig. 9c, which implements an in-situ air liquefaction to provide the oxidizer for the rocket (Escher 1992, NRC 1998). LACE systems have the advantage of further reducing the volume of stored oxidizer and, therefore, reducing the oxidizer tank size and weight. This type of engine collects and liquefies a portion of the incoming air in a heat exchanger which utilizes liquid hydrogen fuel in the condenser. Use of this subsystem would require a very compact, lightweight heat exchanger and a method for alleviating fouling and icing in the heat exchanger. In addition, more hydrogen is required to liquefy the air than is necessary for stoichiometric engine operation which would result in fuel-rich operation thereby decreasing the specific impulse unless a thermal sink, such as slush hydrogen, is provided to recycle the excess fuel.

References:

Amin, S. M., and Garris, C. A. J., (1995), “An Experimental Investigation of a Non-Steady Flow Thrust Augmenter,” AIAA Paper 95-2802.

Anderson, G.Y., McClinton, C.R. and Weidner, J.P., (2000), “Scramjet Performance”, in *Scramjet Propulsion*, Progress in Astronautics and Aeronautics, (E.T. Curran and S.N.B. Murthy eds.), vol. 189.

Balempin, V.V., Maita, M. And Murthy, S.N.b., (2000), “Third Way of Development of Single-Stage-to-Orbit Propulsion”, Journal of Propulsion and Power, vol. 16, no. 1., pp. 99-104.

Balepin V.V., Liston, G.L. and Moszée, R.H., (2000), “Combined Cycle Engines with Inlet Conditioning”, 11th AIAA International Space Planes and Hypersonic Systems and Technologies, AIAA 2002-5148.

Bartolotta, P.A, McNellis, N.B. and Shafer, D.G., (2003), “High Speed Turbines: Development of a Turbine Accelerator (RTA) for Space Access”, 12th AIAA International Space Planes and Hypersonic Systems and Technologies, AIAA 2003-6943.

Billig, F. S., Orth, R. C., and Lasky, M., (1968), “Effects of Thermal Compression on the Performance Estimates of Hypersonic Ramjets,” *Journal of Spacecraft and Rockets*, Vol. 5, No. 9, pp. 1076–1081.

Billig, F.S., (1993),”The Integration of the Rocket with the Ram-Scramjet as a Viable Transatmospheric Accelerator,” International Society for Air Breathing Engines, Paper 93-7017.

Billig, F.S., (1996a), “Tactical Missile Design Concepts”, in Tactical Missile Propulsion, Progress in Astronautics and Aeronautics, (G. E. Jensen and D. W. Netzer eds.), vol. 170.

Billig, F. S., (1996b) “Low-Speed Operation of an Integrated Rocket-Ram-Scramjet” in *Developments in High-Speed Vehicle Propulsion Systems*, (S. N. B. Murthy and E. T. Curran eds.), Vol. 165, Progress in Astronautics and Aeronautics, AIAA, pp.51– 104.

Bowcutt, K.G., (2001), “Multidisciplinary Optimization of Airbreathing Hypersonic Vehicles”, Journal of Propulsion and Power, vol. 17, no. 6., pp. 1184-1190.

Bowman, H., Gutmark, E., Schadow, K., Wilson, K., and Smith, R., (1990), “Supersonic Rectangular Isothermal Shrouded Jets,” AIAA Paper 90-2028.

Bryson, A. E., Desai, M. N., and Hoffman, W. C., (1969), “Energy-State Approximation in Performance Optimization of Supersonic Aircraft,” *Journal of Aircraft*, vol. 6, no. 6, pp. 481.

Bullock, R.O., (1989), “Design and Development of Aircraft Propulsion Systems”, in *Aircraft Propulsion Systems Technology and Design*, G.C. Oates, ed., AIAA Educational Series, pp. 3-101.

Bulman, M. J., (1993), “Ejector Ramjet,’’ U.S. Patent 5,205,119.

Burakhanov, B.M., Likhachev, A.P., Medin, S.A., Novikov, V.A., Okunev, V.I., Rickman, V.Yu and Zeigarnik, V.A., (2001), “Advancement of Scramjet Magnetohydrodynamic Concept”, *Journal of Propulsion and Power*, vol. 17, no. 6., pp. 1247-1252.

Czysz, P. and Murthy, S.N.B., (1995), “Energy Management and Vehicle Synthesis”, in *Developments in High-Speed-Vehicle Propulsion Systems*, Progress in Astronautics and Aeronautics, (S.N.B. Murthy and E.T. Curran eds.), vol. 165.

Curran, E. T., Heiser, W. H., and Pratt, D. T., (1996), “Fluid Phenomena in Scramjet Combustion Systems,” *Annual Review of Fluid Mechanics*, Vol. 28, pp. 323– 360.

Daines, R. and Segal, C., (1998), “Combined Rocket and Airbreathing Propulsion Systems for Space-Launch Applications”, *Journal of Propulsion and Power*, vol.14, no. 5, pp. 605-612.

Daines, R., and Merkle, C., (1995), “Computational Analysis of Mixing and Jet Pumping in Rocket Ejector Engines,” AIAA Paper 95-2477.

Daines, R., and Bulman, M., (1996), “Computational Analyses of Dynamic Rocket Ejector Flow. elds,” AIAA Paper 96-2686.

Dykstra, F., Caporicci, M., and Immich, H., (1997)‘‘Experimental Investigation of the Thrust Enhancement Potential of Ejector Rockets,’’ AIAA Paper 97-2756.

Escher, W.J.D., and Flornes, B., (1966) ‘‘A Study of Composite Propulsion Systems for Advanced Launch Vehicle Applications,’’ The Marquardt Corp., NAS7-377 Final Rept., Van Nuys, CA.

Escher, W. J. D., (1992) “Cryogenic Hydrogen-Induced Air-Liquefaction Technologies for Combined-Cycle Propulsion Applications,” Rocket Based Combined Cycle (RBCC) Propulsion Technology Workshop, NASA CP-10090, pp. 1– 19.

Escher, W., and Schnurstein, R., (1993), “A Retrospective on Early Cryogenic Primary Rocket Subsystem Designs as Integrated into Rocket-Based Combined-Cycle (RBCC) Engines,” AIAA Paper 93-1944.

Escher, W.J.D., Hyde, E., and Anderson, D., (1995)‘‘A User’s Primer for Comparative Assessments of All-Rocket and Rocket-Based Combined-Cycle Propulsion Systems for Advanced Earth-to-Orbit Space Transportation”, AIAA Paper 95-2474.

Escher, W. J. D. ed., (1997) *The Synerjet Engine*, Progress in Technology, PT-54, Society of Automotive Engineers.

Ferri, A, (1973), “Mixing Controlled Supersonic Combustion”, *Annual Review of Fluid Mechanics*, vol. 5, no. 38.

Foster, R., Escher, W., and Robinson, J., (1989)‘‘Studies of an Extensively Axisymmetric Rocket Based Combined Cycle (RBCC) Engine Powered SSTO Vehicle,’’ AIAA Paper 89-2294.

Georgiadis, N. J., Walker, J. F., and Trefny, C. J., (1998), ‘‘Parametric Studies of the Ejector Process Within a Turbine-Based Combined- Cycle Propulsion System,’’ AIAA Paper 98-0936, Jan. 1998.

Ganji, A. R., Khadem, M., and Khandani, S. M., (1991), ‘‘Turbo/Air- Augmented Rocket: A Combined Cycle Propulsion System,’’ *Journal of Propulsion and Power*, Vol. 7, No. 4, pp. 650– 653.

Gregory, D.C. and Han, S., (2003), “Effects of Multiple Primary Flows on Ejector Performance in an Ejector-Ram Rocket Engine”, AIAA 2003-373.

Guoskov, O.V., Kopchenov, V.I., Lomkov, K.E., Vinogradov, V.A., Waltrup, P.J. (2001) ”Numerical Researches of Gaseous Fuel Pre-Injection in Hypersonic 3-D Inlet”, *Journal of Propulsion and Power*, vol.17, no. 6, pp.1162-1169.

Gusev, V. N., (1995),“Optimal Aerodynamic Shapes of a Hypersonic Vehicle with an Airbreathing Engine”, in *Developments in High-Speed-Vehicle Propulsion Systems*, Progress in Astronautics and Aeronautics, (S.N.B. Murthy and E.T. Curran eds.), vol. 165.

Hargraves, C.R. and Paris, S.W., (1987), “Direct Trajectory Optimization Using Nonlinear Programming and Collocation”, *Journal of Guidance*, vol. 10, no. 4.

Heiser, W. H. and Pratt, D.T., (with Daley, D.H. and Mehta, U.B.,1994) *Hypersonic Airbreathing Propulsion*, AIAA Educational Series.

Ho, C.-H., and Gutmark, E., (1987), “Vortex Induction and Mass Entrainment in a Small-Aspect-Ratio Elliptic Jet,” *Journal of Fluid Mechanics*, vol. 179, pp. 383– 405.

Kim, J.-H., Samimy, M., and Erskine, W. R., (1998), “Mixing Enhancement with Minimal Thrust Loss in a High Speed Rectangular Jet,” AIAA Paper 98-0696.

Leingang, J., (1992), “Advanced Ramjet Concepts Program”, Rocket Based Combined Cycle (RBCC) Propulsion Technology Workshop, NASA CP-10090, pp. 1– 9.

Lockwood, R., and Patterson, W., (1962), “Energy Transfer from an Intermittent Jet to a Secondary Fluid in an Ejector-Type Thrust Augmenter,” Hiller Aircraft Co., Rept. ARD-305, Newark, CA.

"Maintaining US Leadership in Aeronautics. Breakthrough Technologies to Meet Future Air and Space Transportation and Goals", (1998), National Research Council, *National Academy Press*.

Marchand, A.P., Kruger, H.G., Power, T.D. and Segal, C., (2002), "Synthesis and Properties of Polycyclic Cage Hydrocarbons (High Energy Density Fuels) and of Polycyclic Cage Organonitro Compounds (Insensitive High-Energy Explosives)" Kem. Ind. 51, pp. 51-67.

Mattingly, J.D., Heiser, W.H. and Pratt, D.T., (2002), *Aircraft Engine Design*, 2nd ed. AIAA Educational Series.

Mehta, U.B. and Bowles, J.V., (2001), "Two-Stage-to-Orbit Space plane Concept with Growth Potential", *Journal of Propulsion and Power*, vol.17, no. 6, pp. 1149-1161.

Oran, E.S, (2001), *Numerical Simulation of Reactive Flow*, Cambridge Univ. Press, 2nd ed.

Ortwerth, P.J. (2000), "Scramjet Flowpath Integration", in *Scramjet Propulsion*, Progress in Astronautics and Aeronautics, (E.T. Curran and S.N.B. Murthy eds.), vol. 189.

Liou, T., Chen, L., and Wu, Y., (1993), "Effects of Momentum Ratio on Turbulent Nonreacting and Reacting Flows in a Ducted Rocket Combustor," *International Journal of Heat and Mass Transfer*, vol. 36, no. 10, pp. 2589– 2599.

Mitani, T., Hiraiwa, T., Tarukawa, Y. And Masuya, G. (2002), "Drag and Total Pressure Distribution in Scranjet Engines at Mach 8 Flight", *Journal of Propulsion and Power*, vol.18, no. 4, pp.953-960.

Palaszewski, B., Ianovski, L. S., and Carrick, P., (1997),"Propellant Technologies: A Persuasive Wave of Future Propulsion Benefits," *Proceedings of the 3rd International Symposium on Space Propulsion,* (V. Yang, G. Liu, W. Anderson, and M. Habiballah eds.), The Chinese Society of Astronautics, Beijing, PRC, pp. 1 – 13.

Presz, W., Morin, B., and Gousy, R., (1988), "Forced Mixer Lobes in Ejector Designs," *Journal of Propulsion and Power*, Vol. 4, No. 4, pp. 350– 354.

Riggins, D.W., (1997) "Thrust Losses in Hypersonic Engines Part 2: Applications", *Journal of Propulsion and Power*, vol.13, no. 2, pp. 288-295.

Rohde, J., (1992),"Airbreathing Combined Cycle Engine Systems," Rocket Based Combined Cycle (RBCC) Propulsion Technology Workshop, NASA CP-10090, pp. 1– 9.

Schmidt, D.K., (1997), "Optimum Mission Performance and Multivariable Flight Guidance for Airbreathing Launch Vehicles", Journal of Guidance, Control and Dynamics, vol. 20, no. 6, pp. 1157-1164.

Schmidt, D.K. and Hermann, J.A., (1998), "Use of Energy-State Analysis on a Generic Air-Breathing Hypersonic Vehicle", Journal of Guidance, Control and Dynamics, vol. 21, no. 1, pp. 71-76.

Segal, C., Friedauer, M. J., Udaykumar, H. S., and Shyy, W., (1995), "Combustion of High-Energy Fuels in High Speed Flows,'' *Proceedings of the 8th ONR Propulsion Meeting*, (G. D. Roy and F.A. Williams eds.), pp. 192– 199.

Segal., C., and Shyy, W., (1996), "Energetic Fuels for Combustion Applications," *Journal of Energy Resources Technology*, Vol. 118, No.3, pp. 180– 186.

Semenov, V.L., Prokhorov, A.N., Strokin, M.V., Relin, V.L. and Alexandrov, V.Yu., (2002), "Fire Tests Of Experimental Scramjet In Free Stream In Continuously

Working Test Facility”, http://hypersonic2002.aaaf.asso.fr/papers/Semenov_paper.pdf.

Siebenhaar, A., and Bulman, M., (1995) “The Strutjet Engine: The Overlooked Option for Space Launch”, AIAA Paper 95-3124.

Sosounov, V. S., Tskhovrebov, M. M., Solonin, V. I., Kadjardousov, P. A., and Palkin, V. A., (1996), ‘‘Turboramjets: Theoretical and Experimental Research at Central Institute of Aviation Motors,’’ Developments in High-Speed Vehicle Propulsion Systems, S. N. B. Murthy and E. T. Curran eds., Vol. 165, Progress in Astronautics and Aeronautics, AIAA, pp. 205– 258.

Steffen, C. J., Jr., Smith, T. D., Yungster, S., and Keller, D. J., (1998), “Rocket Based Combined Cycle Nozzle Analysis Using NPARC,” AIAA Paper 98-0954.

Stroup, K., and Pontzer, R., (1968), “Advanced Ramjet Concepts, Volume I. Ejector Ramjet Systems Demonstration,” The Marquardt Corp., Air Force Aero Propulsion Lab., TR-67-118.

Trefny, C.J., (1999), “An Air-Breathing Launch Vehicle Concept for Single-Stage-to-Orbit”, NASA TM- 209089.

Vinogradov,V, Segal,C, Owens.M and Mullargili.S (2001) “Effect of Kerosene Preinjection on Combustion Flameholding in a Mach 1.6 Airflow”, *Journal of Propulsion and Power* vol.17, no. 3, pp. 605-611.

Warnatz, J., Maas, U. and Dibble, R.W., (1996), *Combustion – Physical and Chemical Fundamentals, Modeling and Simulation, Experiments, Pollutant Formation*, Springer-Verlag.

Yang, V., and Zarko, V. E. eds., (1995), “Solid Propellant Rocket Motor Interior Ballistics and Combustion of Energetic Materials,” Special Issue of *Journal of Propulsion and Power*, Vol. 11, No. 4.

Younghans, J.L., (1989), “Inlets and Inlet/Engine Integration”, in *Aircraft Porpulsion Systems Technology and Design*, G. C. Oates, ed., AIAA Educational Series.